Angular distributions in the electron impact excitation of Xe at 20 eV

W. Williams*, S. Trajmar*, and A. Kuppermann†

California Institute of Technology, Pasadena, California 91109
(Received 22 November 1974)

Electron impact energy-loss spectra of Xe have been studied at 20 eV incident electron energy from 5° to 135° scattering angle. Differential and integral cross sections for elastic scattering and for the excitation of electronic states up to 10.60 eV energy loss have been determined. The validity of the optical selection rules and the previously established angular behavior associated with direct and exchange processes were examined for this intermediate coupling case.

I. INTRODUCTION

It has been previously observed that in the case of atomic and molecular systems whose energy levels can be well described by the L, S coupling scheme, a correlation exists between the shape of the angular distributions of inelastically scattered electrons and the spin multiplicity of the upper and lower states associated with the excitation process.[1,2] In particular, it was observed that for optically allowed transitions, at impact energies of about 10 eV or higher above threshold, the angular distributions show a sharp forward peaking. For processes which are optically spin-forbidden but symmetry-allowed, the distributions are nearly isotropic. An interpretation of this behavior is that optically allowed transitions occur predominantly via long range coulombic interactions, whereas spin-forbidden transitions occur via short range exchange interactions.

An interesting question is what are the characteristics of the angular distributions of electrons inelastically scattered off systems for which spin angular momentum is not a good constant of the motion. Does one still have widely diverse types of angular distributions, and if so, can they still be correlated with the effective range of the different kinds of interactions? To approach these questions, we have chosen to study xenon, which is an important laser material and an atom for whose excited states the spin angular momentum is a very poor constant of the motion.

There is only a small amount of experimental work on the electron impact excitation of Xe. A summary of the older work has been given by Kieffer[3] and by Massey and Burhop.[4]

Energy-loss studies at 90 eV electron impact energy and 0° have been carried out by Simpson *et al.*[5] They found indications for the presence of optically forbidden transitions in the ionization continuum. Kuyatt[6] observed only optically allowed transitions at the same impact energy and scattering angle in the 8 to 13 eV energy-loss region. More recently, Swanson *et al.*[7] measured differential excitation functions from near threshold to 12 eV impact energy for the $6s$ and $6s'$ states at 45°.

Kuyatt *et al.*[8] detected resonances in the elastic electron scattering from Xe and Sanche and Schulz[9] have observed structure in the total cross section from 8 to 13 eV in an elegant transmission experiment.

We report here differential and integral cross sections for the excitation of Xe up to 10.60 eV energy loss at 20 eV impact energy.

II. EXPERIMENTAL

The experimental apparatus has been briefly described in an earlier publication.[10] An energy-selected electron beam with initial kinetic energy $E_0 = 20$ eV was scattered by an atomic beam of Xe. The resulting electron scattering intensity over a small solid angle (10^{-3} sr) was measured at a given scattering angle (θ) in the angular range from 5° to 135° as a function of energy loss (ΔE). An energy-loss spectrum was obtained by the superposition of many scans with a multichannel scaler.

The impact energy scale was calibrated by mixing He and Xe and locating the 19.36 eV He resonance to determine the magnitude of any contact potential. The instrumental resolution was about 0.05 eV and the scattering angles were accurate to ±1°. The angular resolution is estimated to be between 1.7 and 3.2°.[11] Examples of the energy-loss spectra are shown in Fig. 1.

The relative scattering intensities associated with elastic and inelastic processes up to 10.6 eV were determined at various scattering angles. From the elastic scattering intensity and the appropriate volume corrections for our scattering geometry, the elastic differential cross section (DCS) in arbitrary units from 10° to 135° was determined in a time short compared to the instrumental drift. From the inelastic to elastic intensity ratio and the elastic DCS in arbitrary units at a given angle, the inelastic DCS in the same arbitrary units were obtained. In a similar manner utilizing the scattering intensity distribution of the 8.437 eV $6s$ transition in the $-10°$ to $-5°$ and $+5°$ to $+30°$ region, the differential cross sections for the inelastic processes were obtained in the same arbitrary units. This procedure also served to determine the actual zero scattering angle from the symmetry of the scattering intensity around 0°. These cross section curves were extrapolated to 0° and 180° and then integrated to obtain integral cross sections. The total electron-Xe cross section for 20 eV electrons has been measured previously,[12] as well as the ionization cross section.[13] We have normalized our cross sections to these results. To that effect, it was necessary to estimate the contribution to the total cross section at 20 eV impact energy of energy loss processes beyond the 10.6 eV limit adopt-

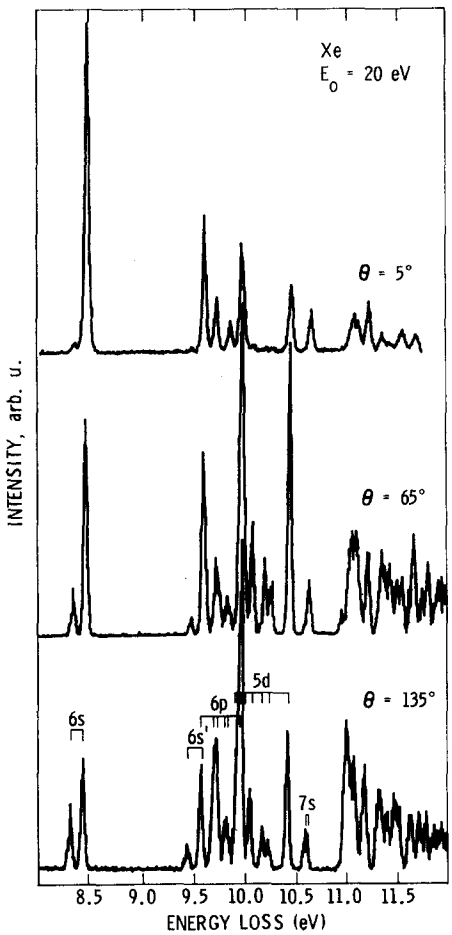

FIG. 1. Energy-loss spectra of Xe at 20 eV impact energy at 5°, 65°, and 135° scattering angles.

ed in most of the present experiments. This estimate was made by obtaining a few energy loss spectra over an energy-loss range extending to the full 20 eV. The integral cross sections Q are listed in Table I and the DCS's are given in Figs. 2–5. The cross sections are estimated to be accurate to ± 50% with $\frac{2}{3}$ of the error attributed to the normalization procedure. The procedure for the error estimation has been discussed in a previous paper.[11] The configuration and term designations, and the energy levels in Table I and in the figures are taken from Moore's[14] tables.

III. COUPLING SCHEMES

The angular momentum coupling in the ground and excited state configurations of elements with low and medium atomic numbers is usually best described in the L, S coupling scheme. Here, the orbital–orbital and spin–spin interactions between the electrons dominate. In such cases, transitions between states of different spin multiplicity can only occur by electron exchange. The exchange interaction is necessarily short-ranged, so one would expect a nearly isotropic distribution of scattered electrons. Indeed, in electron impact spectroscopy, spin-forbidden transitions usually give nearly isotropic electron scattering distributions. Optically allowed transitions, on the other hand, usually give forward-peaked electron scattering distributions when the electron impact energy is at least 10 eV above threshold.

For atoms with high atomic numbers, the spin–orbit interactions between the electrons predominate, and in this case the total angular momentum is best described by the j,j coupling scheme.

In most cases, the coupling situation lies somewhere between the above extremes and it changes not only from one element to another, but from one excited state to the other for the same element. The Xe ground state has the configuration:

$$1s^2 2s^2 2p^6 3s^2 3p^6 3d^{10} 4s^2 4p^6 4d^{10} 5s^2 5p^6;\ ^1S_0\ .$$

Excited states are formed by promoting a $5p$ electron into higher orbitals. The excited neutral states thus formed are customarily described in terms of an $(N-1)$ electron core and the excited electron. In this scheme, two series of lines are expected, one associated with the $^2P_{3/2}$ and the other with the $^2P_{1/2}$ ion core, and they are designated as nl and nl', respectively. The optical spectrum of Xe^+ shows a large energy separation of the $^2P_{3/2}$ and $^2P_{1/2}$ states which indicates a strong spin–orbit interaction in the Xe^+ core. The coupling in excited Xe is usually described in terms of the J, l coupling scheme suggested by Racah.[15] This scheme is based on the fact that the electrostatic interaction between the core and the excited electron is more important than the outer electron's spin–orbit interaction. The resultant angular momentum J_c of the core vectorially couples with the orbital angular momentum l of the excited electron to yield K which in turn couples with the spin s of the outer electron to give the total angular momentum J: $[(J_c, l)K, s]J$. For example, in this scheme, the $6s$, $J=1$ (8.437 eV) transition is represented by $[J_c = 3/2,$

TABLE I. Integral cross sections and angular distributions.

Config.	J	eV	ΔJ[a]	$Q(10^{-16}$ cm$^2)$	Expt.[b]
$5p^6$	0	0.000		14.00	FP
$5p^5(^2P_{3/2})6s$	2	8.315	−	0.0062	WFP
$5p^5(^2P_{3/2})6s$	1	8.437	+	0.0400	FP
$5p^5(^2P_{1/2})6s'$	0	9.447	−	0.0034	WFP
$5p^5(^2P_{1/2})6s'$	1	9.570	+	0.0280	FP
$5p^5(^2P_{3/2})6p$	1	9.580	+		
$5p^5(^2P_{3/2})6p$	2	9.686	−	0.0148	FP
$5p^5(^2P_{3/2})6p$	3	9.721	−		
$5p^5(^2P_{3/2})6p$	1	9.789	+	0.0072	FP
$5p^5(^2P_{3/2})6p$	2	9.821	−		
$5p^5(^2P_{3/2})5d$	0	9.891	−		
$5p^5(^2p_{3/2})5d$	1	9.917	+		
$5p^5(^2P_{3/2})6p$	0	9.934	−	0.0550	WFP
$5p^5(^2P_{3/2})5d$	4	9.943	−		
$5p^5(^2P_{3/2})5d$	2	9.959	−		
$5p^5(^2P_{3/2})5d$	3	10.039	−	0.0152	NIS
$5p^5(^2P_{3/2})5d$	2	10.158	−	0.0079	NIS
$5p^5(^2P_{3/2})5d$	3	10.220	−	0.0052	NIS
$5p^5(^2P_{3/2})5d$	1	10.401	+	0.0320	WFP
$5p^5(^2P_{3/2})7s$	2	10.562	−	0.0079	FP
$5p^5(^2P_{3/2})7s$	1	10.593	+		

[a] + selection rule obeyed; − selection rule not obeyed; bracketed lines were not resolved in the present work.
[b] FP—forward-peaked DCS; WFP—weakly forward-peaked; NIS—nearly isotropic.

$l=0)\,K=3/2,\ s=1/2]\,J=1$.

IV. RESULTS

Typical angular distributions for scattered electrons are shown in Fig. 2. The elastic cross section shows very pronounced structure. Distinct minima in the DCS are present at 50° and 100° scattering angles. Angular distributions for inelastic scattering vary from strongly forward-peaked to nearly isotropic.

A. 6s, 6s′, and 7s states

The DCS's for the 6s, 6s′, and 7s states from 0° to 140° scattering angles are shown in Fig. 3. The 6s, $J=1$ (8.437 eV) and the composite (unresolved) [6s′, $J=1$ (9.570 eV) + 6p, $J=1$ (9.580 eV)] features have forward-peaked electron scattering distributions. In contrast, the 6s, $J=2$ (8.315 eV) and 6s′, $J=0$ (9.447 eV) transitions are slightly forward-peaked, have quite similar scattering distributions and possess shallow minima at a scattering angle around 70°.

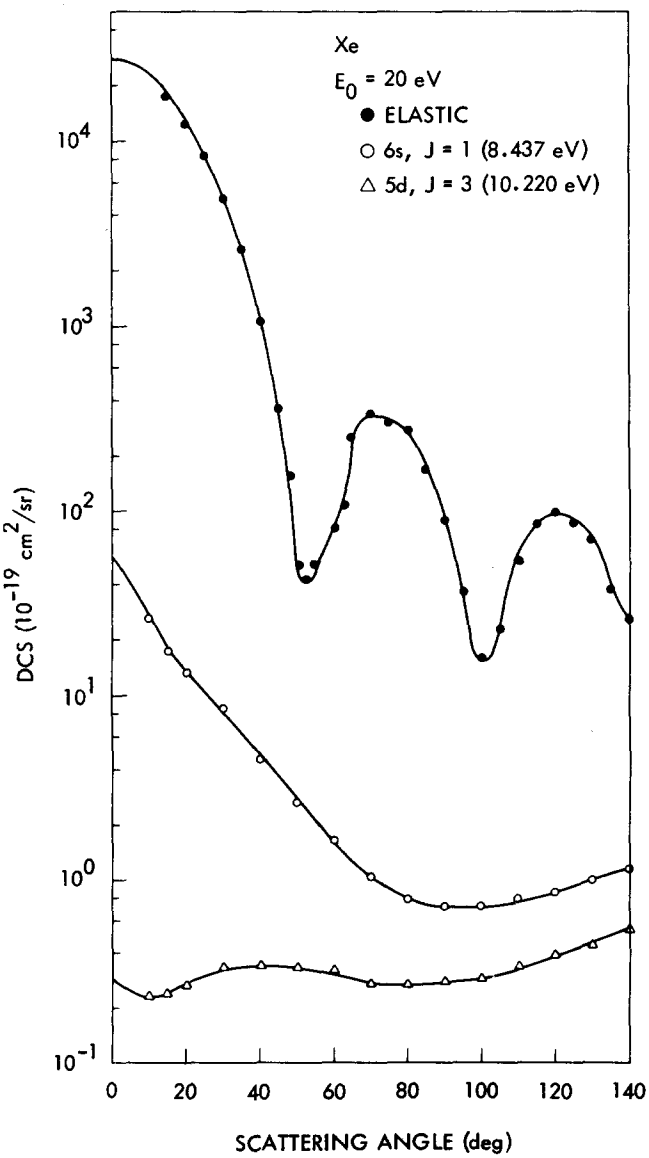

FIG. 2. Differential cross sections for elastic scattering and for excitation of the 8.437 6s and 10.220 eV 5d states.

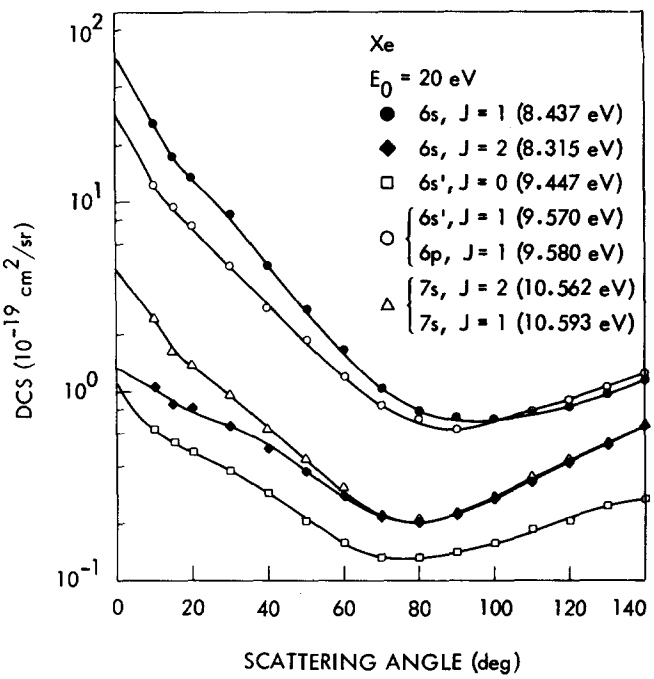

FIG. 3. Differential cross sections for the 6s, 6s′, and 7s excitations.

The 7s levels at 10.562 and 10.593 eV were not resolved in these series of experiments, but the composite transition [7s, $J=2$ (10.562 eV) + 7s, $J=1$ (10.593 eV)] has a forward-peaked electron scattering distribution.

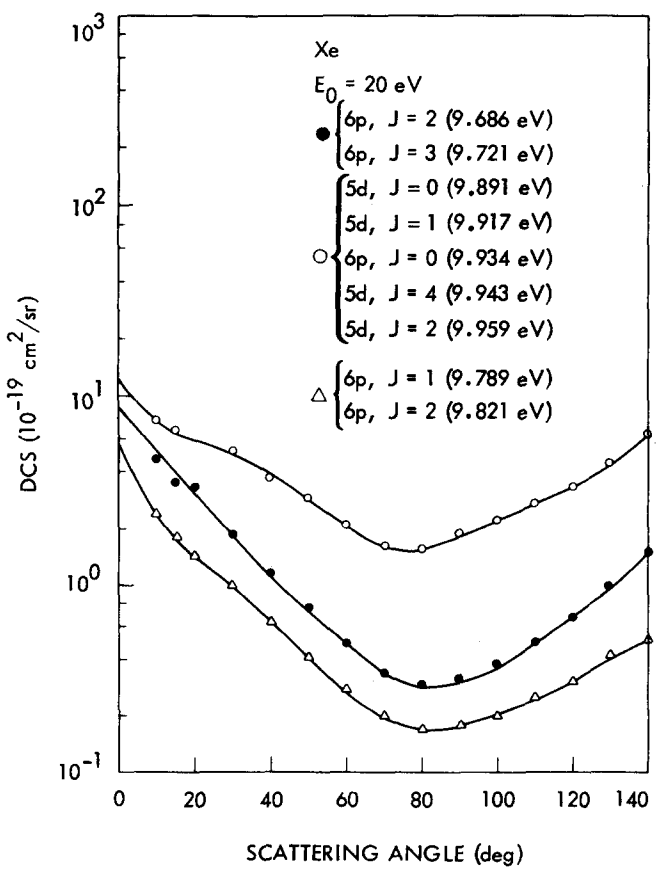

FIG. 4. Differential cross sections for the 6p excitations.

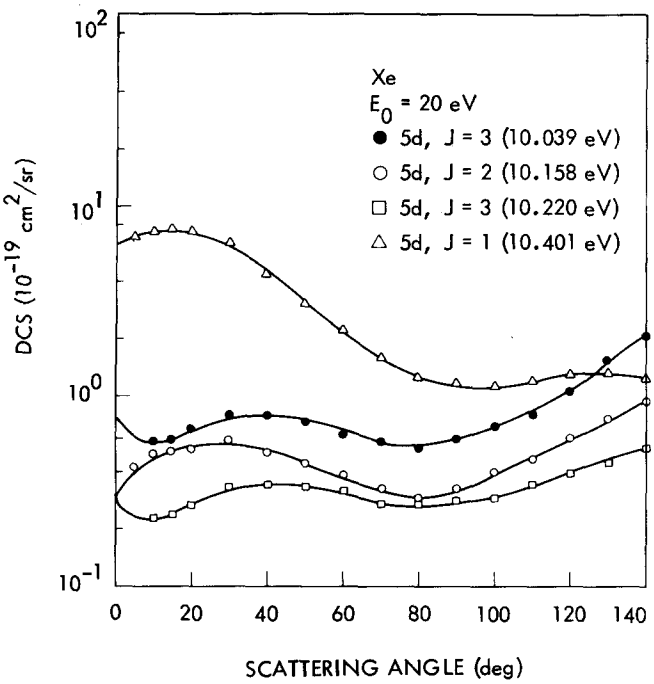

FIG. 5. Differential cross sections for the 5*d* excitations.

At low scattering angles, most of the observed feature is due to the excitation of the 7*s*, $J=1$ (10.593 eV) state since the composite feature is found experimentally at 10.59 eV. At high scattering angles the feature shifts to 10.57 eV implying a more equal contribution of both transitions. Therefore, the 7*s*, $J=1$ (10.593 eV) transition is principally responsible for the forward-peaking.

B. 6*p* states

None of the individual 6*p* excitations are resolved in the present experiments. The 6*p* (9.580 eV) and 6*s*′ (9.570 eV) transitions are mixed as mentioned above. The 6*p* level at (9.934 eV) is overlapped by four 5*d* levels and the resolution was not good enough to separate the remaining two pairs of levels. The DCS's for the [6*p*, $J=2$ (9.686 eV) + 6*p*, $J=3$ (9.721 eV)], [6*p*, $J=1$ (9.789 eV) + 6*p*, $J=2$ (9.821 eV)] and [6*p*, $J=0$ (9.934 eV) + four 5*d* levels] states are shown in Fig. 4. The first two DCS's are forward-peaked while the 6*p* composite at 9.934 eV is slightly forward-peaked. The three spectral features possess minima at 80° scattering angle.

C. 5*d* states

As mentioned above, four of the 5*d* states overlap the 6*p* level at 9.934 eV. The remaining four 5*d* transitions, however, were resolved and their DCS's are plotted in Fig. 5. The 5*d*, $J=3$ (10.039 eV), 5*d*, $J=2$ (10.158 eV), and 5*d*, $J=3$ (10.220 eV) levels have nearly isotropic scattering distributions up to 100° scattering angle. The 5*d*, $J=1$ (10.401 eV) transition is slightly forward-peaked.

D. Integral cross sections

The integral cross sections Q for all observed excitations are presented in Table I.

V. DISCUSSION

The ground state of Xe is designated $^1S_0$ by Moore,[14] implying that S and L are good quantum numbers. Although the excited states are best described by the intermediate J, l coupling scheme, the total angular momentum remains a good constant of the motion for both ground and excited states and the dipole selection rule $\Delta J=+1$ applies to these excitations.[16] One would expect that this ΔJ optical selection rule would apply to electron impact excitations at high impact energies and low scattering angles as the momentum transfer approaches zero.[17]

Abbink and Dorgelo[18] have obtained vacuum ultraviolet absorption spectra of xenon. They report observation of the 6*s*, $J=1$ (8.437 eV), the 6*s*′, $J=1$ (9.570 eV), the 5*d*, $J=1$ (9.917 eV), and the 5*d*, $J=1$ (10.401 eV) transitions which is in accordance with the ΔJ selection rule. It is interesting that they do not report any 6*p* excitation, not even the 6*p*, $J=1$.

Kuyatt *et al.*[6] studied xenon at 0° and 100 eV impact energy, an energy and angle that preferentially select optically allowed transitions. Four levels dominate in their spectrum; the 6*s*, $J=1$ (8.437 eV), the composite (unresolved) [6*s*′ $J=1$ (9.570 eV) + 6*p*, $J=1$ (9.580 eV)], the 7*s*, $J=1$ (10.592 eV) and the 5*d*, $J=1$ (10.401 eV) transition which is by far the most intense. The [6*p*, $J=2$ (9.686 eV) + 6*p*, $J=3$ (9.721 eV)] feature which is large in our low angle 20 eV spectra is small in the 0°, 100 eV spectrum by comparison to the $J=1$ transitions.

An examination of Figs. 2–5 show that transitions with $\Delta J=1$ have the largest cross sections and show forward-peaked electron scattering distributions. There is one exception, however, the composite (unresolved) [6*p*, $J=2$ (9.686 eV) + 6*p*, $J=3$ (9.721 eV)] is large and forward-peaked implying the ΔJ selection rule does not apply for this transition at intermediate energies.

VI. SUMMARY AND CONCLUSIONS

A variety of angular distributions have been observed for the electron impact excitation of xenon. We find that the ΔJ selection rule shows its effect even at intermediate energies and there seems to be some correlation between the angular distribution and the ΔJ optical selection rule. The ΔJ allowed transitions have large and forward peaking differential cross sections, while the ΔJ forbidden ones are weaker and more isotropic. These conclusions refer to the 6*s*, 6*s*′, and 7*s*, and 5*d* excitations. Excitations of the 6*p* levels are absent in the optical limit and the ΔJ selection rule does not seem to apply to these excitations at intermediate energies. An explanation of these observations constitutes a theoretical challenge.

ACKNOWLEDGMENT

We wish to thank Dr. C. E. Kuyatt's laboratory for providing us with a 0°, 100 eV energy loss spectrum of xenon and Dr. A. Chutjian for helpful discussions concerning the measurements.

*Jet Propulsion Laboratory work supported by the National Aeronautics and Space Administration under Contract No. NAS7-100.

†A. A. Noyes Laboratory of Chemical Physics, Division of Chemistry and Chemical Engineering. Contribution No. 4995. Work supported in part by U. S. Atomic Energy Commission, Report Code No. CALT-133.

[1]A. Kuppermann, J. K. Rice, and S. Trajmar, J. Phys. Chem. 73, 3894 (1968).

[2]S. Trajmar, J. K. Rice, and A. Kuppermann, Adv. Chem. Phys. 18, 15 (1970).

[3]L. J. Kieffer, At. Data 1, 121 (1969); 2, 293 (1971).

[4]H. S. W. Massey and E. H. S. Burhop, *Electronic and Ionic Impact Phenomena* (Clarendon, Oxford, 1969), Vol. I, pp. 334.

[5]J. A. Simpson, S. R. Mielczarek, and J. Cooper, J. Opt. Soc. Am. 54, 269 (1964).

[6]C. Kuyatt, Natl. Bureau of Standards (private communication).

[7]N. Swanson, R. J. Celotta, and C. E. Kuyatt, VIII International Conference on the Physics of Electron and Atomic Collisions, Belgrade, Yugoslavia, 1973, Abstracts (Institute of Physics, Beograd, Yugoslavia, 1973), p. 478.

[8]C. E. Kuyatt, J. A. Simpson, and S. R. Mielczarek, Phys. Rev. 138, A 385 (1965).

[9]L. Sanche and G. J. Schulz, Phys. Rev. A 5, 1672 (1972).

[10]A. Chutjian, D. C. Cartwright, and S. Trajmar, Phys. Rev. Lett. 30, 195 (1973).

[11]S. Trajmar, Phys. Rev. A 8, 191 (1973).

[12]H. S. W. Massey and E. H. S. Burhop, *Electronic and Ionic Impact Phenomena* (Clarendon, Oxford, 1969), Vol. I, p. 25.

[13]D. Rapp and P. Englander-Golden, J. Chem. Phys. 43, 1464 (1965).

[14]C. Moore, *Atomic Energy Levels* 3, 113 (1958).

[15]G. Racah, Phys. Rev. 61, 537 (1942).

[16]E. V. Condon, and G. H. Shortley, *The Theory of Atomic Spectra* (Cambridge University, Cambridge, 1959), pp. 303.

[17]E. N. Lassettre, A. Skerbele, and M. A. Dillon, J. Chem. Phys. 50, 1829 (1969).

[18]J. Abbink and H. Dorgelo, Z. Phys. 47, 221 (1928).